ANSTO/E712

ANSTO/E712

ansto

GENERATION AND VALIDATION OF A CROSS SECTION LIBRARY BASED ON ENDF/B-VI FOR THE AUS NEUTRONICS CODE SYSTEM

by

G. S. ROBINSON

December 1993

ISBN 0 642 59950 5

ISSN 1030-7745

REPORT

AUSTRALIAN NUCLEAR SCIENCE
AND TECHNOLOGY ORGANISATION

LUCAS HEIGHTS RESEARCH LABORATORIES

GENERATION AND VALIDATION OF A CROSS SECTION LIBRARY BASED ON ENDF/B-VI FOR THE AUS NEUTRONICS CODE SYSTEM

by

G. S. Robinson

ABSTRACT

The generation of a cross section library with 200 neutron and 37 photon groups from ENDF/B-VI for use in the AUS modular neutronics code system is described. The NJOY code was used for most of the library preparation but a revision of previous AUS methods was used for the neutron resonance treatment. The library should be suitable for thermal and fast fission reactors, fusion blankets and various neutron applications. The validity of AUS with the library was established for thermal and fast reactor systems by an extensive set of comparisons with benchmark experiments which were mainly taken from the ENDF compilation. The performance of AUS with the library was much improved over that with the previous ENDF/B-IV based library.

ISBN 0 642 59950 5
ISSN 1030-7745

The following descriptors have been selected from INIS Thesaurus to describe the subject matter of this report for information retrieval purposes. For further details please refer to IAEA-INIS-12 (INIS: Manual for Indexing) and IAEA-INIS-12 (INIS: Thesaurus) published in Vienna by the International Atomic Energy Agency.

A CODES; ALGORITHMS; BENCHMARKS; COMPARITIVE EVALUATIONS; COMPUTER CALCULATIONS; COMPUTER CODES; CROSS SECTIONS; EVALUATED DATA; EXPERIMENTAL DATA; FAST REACTORS; FISSION; KERMA; MULTIGROUP THEORY; NEUTRONS; NUCLEAR DATA COLLLECTION; PHOTONS; REACTOR PHYSICS; RESONANCE; THERMAL REACTORS

EDITORIAL NOTE

The Australian Nuclear Science and Technology Organisation (Ansto) replaced the Australian Atomic Energy Commission (AAEC) on 27 April 1987. Reports issued after April 1987 have the prefix ANSTO with no change of the symbol (E, M, S or C) or the numbering sequence.

1. INTRODUCTION

The AUS modular neutronics code system [1] consists of a number of computer programs which may be linked in a flexible manner and a few associated group cross section libraries. AUS is now written in portable Fortran 77 and currently operates under a UNIX operating system on a Fujitsu VP2200 computer which may be accessed through AARNet and Internet as *photon.ansto.gov.au*. To enable a wide range of calculations to be performed, the libraries include subgroup representation of resonances, scattering matrices dependent on potential scattering, temperature dependence of resonance and thermal data, P_l scattering matrices, kerma data, and an extensive set of nuclides including fission products. The subgroup treatment is applied to resonance scatterers such as Na, Al and Fe as well as to the actinides. Until now the most recent of these libraries was the AUS.ENDF200G library [2] which has 200 neutron groups and 37 photon groups. It is mainly based on ENDF/B-IV but does include data from ENDF/B-V for those nuclides such as fission products and higher actinides for which the ENDF/B-V data were released. The generality of the codes and library have enabled their use for a very wide range of calculations including thermal and fast fission reactors, fusion blankets, shielding and various neutron applications.

A new library *aus/endfb6* has now been generated almost exclusively from ENDF/B-VI in the same group structure as that for AUS.ENDF200G. The methods previously used for library generation [2] [3] have been either replaced or extensively revised. This report describes the generation of the library and provides the results obtained from the validation of AUS with the new library. The validation concentrated on the results obtained for benchmark experiments on thermal and fast reactor assemblies.

2. GENERATION OF THE LIBRARY

2.1. General

Much of the library generation was performed using the NJOY91.38 [4] version of the NJOY nuclear data processing system [5]. This comprehensive package was used for the generation of linearised point cross section files at various temperatures, nuclear heating, thermal neutron scattering processing, and the preparation of infinitely dilute group cross sections and scattering matrices. To maintain consistency with the previous resonance treatment in AUS, the generation of point cross section files in the unresolved resonance range, the solution of the slowing down equation and the extraction of group resonance integrals were performed using local programs which were rewritten to conform to NJOY usage. The final steps of conversion to an AUS cross section file and fitting of subgroup parameters also followed similar principles to that used previously. The following subsections give some detail on each of the above procedures and also cover generation of a pseudo fission product and fission energy release data.

Revision 1 of the ENDF/B-VI evaluated nuclear data files from the US National Nuclear Data Center as distributed by the IAEA Nuclear Data Section [6] has been used throughout. The release conditions concerning notification of ENDF/B-VI usage are reproduced in the AUS output file.

2.2. NJOY Modules Used

The NJOY system contains a large number of modules. The following gives a list of the modules used and their application in this work.

- MODER - Converts ENDF/B files from formatted to binary form.
- RECONR - Constructs an ENDF/B pointwise file on which linear interpolation between points can be used. The use of this type of file is fundamental to NJOY processing. RECONR includes the reconstruction of point data at 0 K from neutron resonance parameters. It has been used for both neutron and gamma interaction files.
- BROADR - Numerically Doppler broadens a RECONR output file for pointwise neutron cross sections.
- HEATR - Calculates pointwise neutron KERMA factors and damage cross sections.
- THERMR - Calculates thermal neutron scattering transfers.
- GROUPR - Generates infinitely dilute multigroup neutron cross sections, neutron scattering matrices and photon production matrices from pointwise files. The output is a multigroup version of an ENDF/B file called a GENDF file.
- GAMINR - Generates multigroup interaction data for photons in a similar fashion to the processing of neutron data by GROUPR.

• MIXR - Combines point cross section files to form a file for an element with several isotopes. This was used only to provide data for Ansto's resonance shielding calculations for elements such as Fe.

2.3. Modifications made to NJOY

A considerable number of modifications to NJOY were made in the course of this work, using the NJOY UPD program. The more significant of these changes are listed here with some discussion given where appropriate. Many of the changes were concerned with improving the performance of NJOY on a computer with a short word length (32 bit) and IBM/370 type number representation. A few of the modifications have been included in later NJOY releases.

The major change was an improvement in resonance reconstruction which allowed use of a more refined energy grid with IBM/370 number representation. To limit refinement of the energy grid, the standard NJOY allows the number of significant decimal digits to be given as input. Values greater than six caused problems on the VP2200. The SIGFIG routine was modified to give the maximum floating point single precision of the hardware for input values greater than six. This required the RECONR and BROADR modules to be modified so that manipulation of the energy grid was in double precision. The accuracy of the modified code is considered in the next section.

To overcome problems with thermal scattering matrices, the BINA routine in GROUPR was changed to double precision and the THERMR routine SIGL was also largely changed to double precision. The floating point arithmetic used for indexing in the LOADA routine was changed to fixed point.

The CSRMAT routine in RECONR was corrected to fix the treatment of duplicate J values for Reich-Moore resonance parameters. The original NJOY91.2 correction did not give the required result that the statistical factors g_J sum to $2l+1$, where l is the angular momentum state.

The incident energy grid in THERMR was extended from 4.5 to 850 eV. This allows the thermal scattering treatment to be extended, which is particularly required for heavier moderators such as graphite at high temperatures. This is considered further in the next section. Several modifications were also made to THERMR to avoid problems with the temperature or the incident energy being outside the range of the ENDF file.

A minor modification to the GROUPR module enabled P_7 scattering matrices to be produced. As there is no input allowing for varying scattering order, the thermal scattering and gamma production were limited to P_3 internally.

Two errors in GROUPR which had serious consequences for gamma production were corrected. The first, introduced in NJOY91.30, gave rubbish for nuclides with photon transition probability arrays. The second gave errors for nuclides with constant photon spectra when more than one photon per reaction was produced, because the spectrum was not being normalised.

2.4. NJOY Input Specification

2.4.1. Accuracy of cross section reconstruction

Several NJOY modules have input parameters which determine the accuracy of the calculation. RECONR is controlled by the parameters ERR, ERRMAX and ERRINT which determine the accuracy of cross sections following resonance reconstruction and linearisation. BROADR is controlled by a similar set of parameters. A limited investigation of the effect of varying ERR and ERRMAX was undertaken at the same time as establishing the accuracy of RECONR plus BROADR using the SIGFIG modifications. The maximum number of significant figures has been used throughout. On the VP2200, this gives a precision which varies from 10^{-6} to 6×10^{-8} as on an IBM/370. Some authors have suggested that 10^{-8} precision in the energy grid may be required for accurate resonance reconstruction at 0 K in some energy ranges. This was checked by comparing NJOY with the LINEAR/RECENT/SIGMA1 set of codes [7] which use double precision internally and 9 decimal digits on formatted files used to transfer data between codes. The accuracy criterion with these codes is more straight forward. A fractional accuracy of 0.001 was used in RECENT and no thinning of the energy grid was performed in SIGMA1.

For ^{238}U, shielded group cross sections at 0 K were compared for two energy ranges in which the loss of significance is greatest. The values chosen for ERR were 0.005 and 0.001 and defaults were used for the

other parameters. The results in Table 1 show differences little more than the ERR values.

Table 1. Comparison of ^{238}U Shielded Group Capture Cross Sections

Energy Range (keV)	σ_H† (barns)	RECENT σ_{cap} (barns)	Difference using RECONR (Per cent)	
			ERR=0.005	ERR=0.001
9.12-8.05	∞	0.6598	0.67	0.11
9.12-8.05	20	0.3011	0.81	0.16
4.31-3.80	∞	1.2207	0.24	0.07
4.31-3.80	20	0.3724	0.42	0.12

† Hydrogen scattering per ^{238}U atom.

Comparisons of point cross sections were made for ^{52}Cr at 0 K and 296 K as this was thought to be another nuclide with energy grid problems. Comparisons are of total cross section unless otherwise stated. The first NJOY calculation used ERR of 0.001 and ERRMAX of 0.01 (compared to the default of 20×ERR). This gave differences between RECONR and RECENT of 3.3% at one cross section minima with several other differences of about 1%. The differences at 296 K between BROADR and SIGMA1 were about half as much. The second NJOY calculation used ERRMAX reduced to 0.001. This removed the differences at the minima. There were seven resonances with differences between RECONR and RECENT of around 0.5%. These differences disappeared following Doppler broadening to 296 K. The largest error (1%) occurred for the resonance at 68.23 keV which has a 0.4 eV half-width and is in a number range with precision of only 6×10^{-7}. Looking in detail at this resonance showed that the cross sections agreed to better than 0.1% at the single precision energy points. (The comparison was made in double precision using linear interpolation of the NJOY output file.) Comparisons on this resonance after Doppler broadening showed that NJOY was about 0.03% low in total cross section and 0.05% low in capture cross section over much of the resonance.

It was concluded that no errors of any significance were introduced by the single precision energy grid in the NJOY calculation. The point errors at 0 K disappear on Doppler broadening. Any integral effect is vanishingly small. In practice, ERR of 0.005 and default ERRMAX have been used for Au, Ga and all fission products; ERR of 0.003 and default ERRMAX for ^{237}U, ^{238}Pu and the isotopes of Cd, Np, Am and Cm; ERR of 0.001 and default ERRMAX for Mo, Nb and the remaining U and Pu isotopes; ERR of 0.001 and ERRMAX of 0.005 for the remaining nuclides.

2.4.2. Thermal scattering

The accuracy of thermal scattering generation by THERMR is controlled by the three parameters: the number of equi-probable angles, NBIN; the maximum energy for thermal treatment, EMAX; and tolerance, TOL. The effect of these parameters on the average scattering angle, $\bar{\mu}$, and the scalar group flux in an infinite medium, ϕ, was investigated. Most of the tests were done for graphite using either crystal or gas scattering.

Changing NBIN from 4 to 8 had effects less than 0.2% except for changes of up to 4.5% for gas $\bar{\mu}$. Changing TOL from 0.02 to 0.005 gave differences in ϕ of less than 0.4% for crystal and 1% for gas, but differences in $\bar{\mu}$ of less than 2% for crystal and up to 16% for gas. Changing TOL from 0.005 to 0.002 gave differences in ϕ of less than 0.2% for crystal and 0.4% for gas, but differences in $\bar{\mu}$ of less than 0.5% for crystal and up to 5% for gas. For H in H_2O, changing NBIN from 4 to 8 gave differences less than 0.07% in ϕ and up to 1.7% in $\bar{\mu}$ for the lowest energy groups. Changing TOL from 0.02 to 0.005 gave differences of 0.4% in ϕ and up to 4.4% in $\bar{\mu}$; the $\bar{\mu}$ difference increased with decreasing energy. Though some of these effects appear rather strange, NBIN of 8 and TOL of 0.005 have been used throughout.

For a heavy moderator such as graphite, the upper energy of the thermal scattering range is rather important, particularly at elevated temperatures. For graphite gas at 296 K, the discontinuity in ϕ at the upper energy is 3.6% for EMAX of 4 eV and 1.3% for EMAX of 10.7 eV. The discontinuity for EMAX of 10.7 eV increases to 6.4% at 1600 K. To avoid using the ENDF S(α, β) at much higher energies than intended, gas scattering has been used in an energy range joining the normal thermal range and the slowing down range. The upper energy of the gas range has been taken as 62 eV which gives a discontinuity there of 1%

for graphite at 1600 K. The other joining energy has been taken as 5 eV. The results for graphite and D_2O are compared in Table 2 with standard treatments which join directly to the slowing down treatment. ENDF denotes using the data from the ENDF/B file, SD denotes slowing down. The discontinuity in the flux was taken to be the ratio of flux in the first group of an energy range to the average of the two neighbouring groups.

Table 2. Thermal Flux Discontinuity

For graphite at temperature (K) of:	296		600	1600
Case		Discontinuity		
ENDF/gas joined at 5 eV	1.037		1.021	1.006
ENDF/SD joined at 10.7 eV	1.035		1.041	1.070
ENDF/SD joined at 5 eV	1.066			
For D_2O at temperature (K) of:	296	450	600	1000
Case		Discontinuity		
ENDF/gas joined at 5 eV	1.003	1.002	1.002	1.001
ENDF/SD joined at 5 eV	1.011	1.014	1.017	1.023
ENDF/SD joined at 3 eV	1.016	1.022	1.028	1.041

An upper range of 5 eV for the ENDF/B data has been used for all moderators. An upper range of 62 eV for gas scattering has been used for all nuclides, except the actinides for which 3 eV has been used.

2.4.3. Other NJOY input specifications

The weighting used in GROUPR was the VITAMIN E weighting function with a temperature dependent thermal part. This has components of a thermal Maxwellian, 1/E, fission spectrum and fusion peak. The weighting used in GAMINR was 1/E with rolloffs. This appears to be more appropriate for fission reactors than a weighting which is constant in energy.

2.5. Unresolved Resonance Treatment

The unresolved resonance treatment is embodied in the local UNRESL program which contains an extensively rewritten version of the methods used in the generation of previous AUS libraries. UNRESL adds unresolved resonance cross sections to a linearised ENDF/B binary file as produced by NJOY. A ladder of resonance parameters is selected, then used to generate point cross sections at a number of temperatures. The point cross sections are normalised to the infinitely dilute cross section obtained by the standard ENDF/B method [8] in each energy group specified. In practice, the final AUS group boundaries have been used for the normalisation.

Firstly, the infinitely dilute group cross sections for each l,J state are calculated using the standard ENDF/B method of integration over the resonance width distributions. (The GNRL3 subroutine from the RECENT program was used for the integration.) The integration over neutron energy uses interpolation in point cross sections between the points at which the resonance parameters are tabulated. An input option to interpolate in resonance parameters may be used if it is clear that interpolation in cross sections was not the intended use of the parameters.

Next, a ladder of resonances is selected which matches the required cross sections for each l,J state. If a sufficiently accurate ladder for any l,J state for a group cannot be found within an input number of attempts, the best one found is accepted. This matching is performed on the assumption that each resonance in the group is entirely within that group. As well as the set of resonance parameters, a set of renormalisation factors is also obtained which give the required group cross sections.

Finally, the point cross sections are generated using the selected resonance parameters and renormalised as required. The energy points are selected using a technique similar to NJOY to give the cross section at any energy within the specified tolerance when linear interpolation is used. These cross sections then replace the unresolved resonance range on the input ENDF/B file from NJOY. Multiple temperatures may be

included. A tolerance of 1% has been used in practice.

A problem with the UNRESL technique is that, near the upper boundary of the unresolved resonance range, one may be trying to approximate a cross section which is almost energy invariant by a sum over resonances. This requires an extremely large number of resonances in the summation. Therefore, the unresolved resonance treatment of ^{235}U and ^{241}Pu was restricted to energies below 10.33 keV and 19.3 keV respectively. At these energies the resonance shielding at the extreme σ_H of 10 barns was about 2% which is marginally less than that for ^{239}Pu at the upper limit of its unresolved range in ENDF/B-VI. The number of s wave and p+d wave resonances to be included in the summation are input parameters to UNRESL. For each nuclide, they were chosen from test runs comparing the unshielded cross sections obtained for the highest energy group in the unresolved range with the required values. It appeared that there was a small bias (< 0.3%) in the values which could not be removed by increasing the number of resonances. For the three fissile nuclides treated, 200 s wave and 200 p wave resonances were included in the summation and the maximum deviation was 0.45% for ^{235}U. Fewer resonances were required for fertile nuclides and the deviations were smaller.

2.6. Generation of Resonance Data as a Function of σ_H

The generation of group resonance integrals and scattering matrices as a function of the scattering by hydrogen per resonance atom, σ_H, is performed using the GENRI program. The input cross section file may be a linearised ENDF/B file given either in standard ENDF/B format or in binary NJOY form. The program solves the neutron slowing down equation for a mixture of the resonance nuclide and a nuclide with unit mass and constant scattering cross section. Scattering is assumed to be isotropic in the centre-of-mass system. Inelastic scattering is ignored. The solution technique follows that used in NJOY. Additional energy points are added so that there are a minimum of four points in the scattering range of the resonance nuclide. The cross sections and source at each energy are stored in memory, which simplifies the coding considerably compared to the MINIPEARLS program used in generating previous libraries. It is implicitly assumed throughout GENRI that the cross section is linear in energy between the given energies. The assumption actually made in solving for the flux is that $\sigma_s(E)\phi(E)E$ is linear in energy.

In calculating group resonance integrals and transfer cross sections using the calculated flux, the equations used are those given in Appendix B of the two MIRANDA reports [2] [3]. The additional assumptions made about linearity are that $\sigma_a(E)\phi(E)E$ is linear in energy in calculating the resonance escape probability p(E), and $\sigma_x(E)\phi(E)E/p(E)$ is linear in energy in calculating group resonance integrals for any reaction x.

Additional data required for the scattering radius and the variation of $\bar{\nu}$ with energy are taken from the original ENDF/B file if necessary. For resonance scatterers such as Fe, the point cross section files for the isotopes were combined to form the element before input to GENRI.

2.7. Transformation to an AUS file

The combining of a number of NJOY GENDF files, GENRI output and reaction product decay data to form an AUS cross-section file for a single AUS 'nuclide' was performed using the NJOYAUS program. A number of ENDF/B materials may be mixed to form the AUS file. This allows for moderator molecules and elements which have separate data for each isotope in ENDF/B-VI. Thus an AUS 'nuclide' is an isotope, element or molecule on the cross section library. More than one type of thermal scattering may be included on the NJOY files and the required type is selected in the NJOYAUS input. If gas scattering data are available when $S(\alpha, \beta)$ data are selected, then the gas data will be included above 5 eV. A fission spectrum and $\bar{\nu}$-fission cross section are generated using the formulae (42) to (45) of Volume III of the NJOY report [5]. The group weights included on the GENDF file are used as the weighting flux in the formulae, except that the fusion peak is removed. The program allows the user to define mixtures of ENDF/B MT numbers to form gas production cross sections. Any MT numbers may be included as additional reactions on the output AUS file.

For reactions with short lived radioactive products, NJOYAUS may be used to include the decay energy and decay photons. That is the energy deposited locally and the photons emitted when the reaction product decays are added to the kerma factor and photon production of that reaction. The decay data are included in the NJOYAUS input stream. Where possible, they have been taken from the ENDF/B-VI decay files using the DECAYSP program.

For resonance nuclides, the group resonance integrals and P_0 scattering vectors as a function of σ_{II} produced by GENRI are used to replace much of the data from the NJOY file for (n, γ), fission and elastic scattering. The variation with σ_{II} of each element of the P_l elastic scattering vector for l>0 is obtained by multiplying the NJOY data by the shielding factor for the total elastic scattering. For nuclides with atomic mass greater than 100, anisotropy of scattering is of little importance in the resonance range so the P_0 data from GENRI are used for elastic scattering. For lighter nuclides, each P_0 down-scatter element is obtained by multiplying the NJOY data by the shielding factor for that element from GENRI. The self-scatter term is adjusted to maintain the total elastic scattering from GENRI.

For most nuclides, a transport cross section for use in MIRANDA P_0 calculations has been obtained by subtracting the sum of the P_1 vector from the total cross section in NJOYAUS. MIRANDA is the AUS module which uses the AUS cross section library to prepare data which are appropriate for a particular calculation. For the moderators H_2O, D_2O, CH_2 and graphite, the transport cross section has been obtained from a B_1 calculation in MIRANDA for a ^{235}U fission spectrum source in the moderator with an infinitesimal buckling. The output AUS files from MIRANDA were combined with the original AUS file for the moderator using AUSED [9] to form the final moderator file.

2.8. Fitting of Subgroup Parameters

The fitting of subgroup parameters to the resonance integrals was performed using the AUSED module, which is unchanged in principle from that used previously [2] [3] [9]. The retabulation of the scattering matrices as functions of σ_{II} to be functions of effective potential scattering cross section, $\hat{\sigma}_p$, was also performed by AUSED. The main input to AUSED apart from the AUS file from NJOYAUS is the set of average resonance properties required by MIRANDA for each resonance group. Two of these, the average peak height of the resonance $< \sigma_0 >$ and the average resonance width parameter $< 2E_r/\Gamma >$, are required for the λ method which is applied to all resonance nuclides. They define the effective potential scattering. The other two, which give the average position within the group of resonance absorption and fission are only required for actinides for optional use in MIRANDA. All four parameters were obtained using a simple program, LAMPOS, to average the data from either the original ENDF/B-VI files or output files from UNRESL which include unresolved resonance parameters. A rather arbitrary potential scattering is still required in the averaging [3] and values in the range from 50 to 1000 barns have been used for various nuclides. The major problems with the subgroup fitting were the choice of parameters required for wide resonances extending over many groups and the best choice of σ_k in fitting the group resonance integrals I_x by

$$I_x \approx \sum_k \frac{w_k \hat{\sigma}_p}{(\hat{\sigma}_p + \sigma_k)} \quad .$$

Other problems occur where an important p wave resonance is imposed on a background cross section which differs from the standard potential scattering background. Because of these problems, a trial and error approach was required to get good fits. Since more care was taken, better fits were obtained for this library than for previous libraries.

Great care was taken to ensure that the processing of resonance information by GENRI, NJOYAUS, AUSED and MIRANDA was consistent. One improvement made was to eliminate duplication of inelastic scattering data on the AUS library. For scattering vectors which are dependent on potential scattering (and temperature), if the first vector of the set for a group is longer than the rest, it is implied that the additional data of the first vector apply to the other potential scattering and temperature values also.

2.9. Fission Product Treatment

The cross section library includes data for 158 fission products which is two more than on AUS.ENDF200G. This number is rather excessive for those calculations which are only concerned with reactivity related effects of the fission products. Therefore, a pseudo fission product labelled PFP has been generated which replaces 105 of them to give a standard set of 53 main fission products and the pseudo product. (Using the complete set is an option in MIRANDA.) All the fission product yield and decay data have been taken from ENDF/B-VI files. Fission product yields on an AUS library are given for only six fuel types. Currently, these are ^{233}U, ^{235}U, ^{238}U, ^{239}Pu, ^{240}Pu and ^{241}Pu where yields for ^{238}U and ^{240}Pu are for incident neutron energies of 3.35 and 2 MeV respectively and the remainder are thermal yields. Other nuclides use the data for one of these six. For full fission product calculations including heat

generation and gamma production, the file *aus/endf6.fisprodsp* is used in the CHAR module [10] as an additional data source. This file also includes decay heat and gamma spectra for the actinides on the cross section library with half lives less than one thousand years. Again, the data have been taken from ENDF/B-VI files.

The data for PFP were obtained from a simple PWR cell calculation using both sets of 158 and 53 fission products. Results for the total fission product capture rates c_j for each fuel type, j, were obtained as a function of time from calculations in which the fuel type was set, for all fissionable nuclides, to each value of j from one to six in turn. The differences Δc_j between the 158 and 53 fission product sets were well approximated as being proportional to both flux level and time. The cross sections for PFP were obtained by weighting the cross sections of the 105 nuclides to be replaced, by the atom densities after 600 days for the standard calculation. The important quantities are the PFP yields which were obtained from the equation:

$$\bar{y}_j = C \frac{\Delta c_j}{\Delta c_2} \sum_{k>53} y_{i(k),2} \quad ,$$

where C is a normalisation factor,
Δc_j are total captures for the period from 600 to 800 days,
i(k) is a pointer to the yield to use for nuclide k,
$y_{k,j}$ is the yield of nuclide k for fuel type j, and
2 represents the yields from ^{235}U fission.

To assess the accuracy of results with the 53 fission product set plus PFP, the total fission product captures in 200 day periods up to 1000 days for the standard PWR burnup calculation were compared. The reduced set gave errors of 0.27, 0.17, 0.09, 0.00 and -0.10 per cent for the five time periods when compared with the 158 fission product set. The agreement for the 600 to 800 day period is a result of the normalisation. A similar comparison was made for 20 day periods for a cell burnup calculation of HIFAR which is Ansto's 10 MW DIDO class research reactor. This gave errors of 0.38, 0.50, 0.47, 0.42, 0.39 and 0.36 per cent in total fission product captures for six periods up to 120 days. Both sets of results are considerably improved for the initial period over the results of similar comparisons made using AUS.ENDF200G. This is a consequence of including extra short lived fission products in the main set.

2.10. Fission Energy Release

The data on fission kerma on the AUS files were modified from that obtained using NJOY. The major problem with the NJOY data was that a lack of MT 458 data on the ENDF/B-VI files for many nuclides led to an inconsistency. Also, NJOY did not include the dependence of energy release per fission on incident neutron energy. In fact, fission kerma can only be treated accurately by making the data consistent with the fission product yield data and the fission product gamma and beta energy release. The fission kerma factors should include the energy per fission representing just the kinetic energy of the fission fragments plus some minor correction terms. To do this, the fission product energy release per fission using yields for each fuel type was calculated using *aus/endf6.decaysp* for a HIFAR-like cell calculation with ^{235}U the only actinide and ^{235}U not burning out. Then the fission kerma factors were modified using the equivalent of the following change in the energy release per fission from that derived in NJOY. It is based on reference 8 and uses the same notation.

$$\Delta = EGD_{458} + EB_{458} - EGD_j - EB_j + .157EINC + .15EY_j + 8.07 \times 10^{+6}(\bar{\nu}(EINC) - \bar{\nu}(0))$$

where EGD_{458}, EB_{458} are the delayed γ and βenergy subtracted in NJOY if any,
EGD_j, EB_j are the values calculated above for the appropriate set j of fission product yields,
EINC is the incident neutron energy,
EY_j is the incident neutron energy for which the j^{th} set of fission product yields were calculated and this term represents $\delta EGD + \delta EB$, and
the last term represents $\delta\bar{\nu}$.

The fission kerma data may be used in a coupled neutron/photon calculation of the spatial distribution of the energy deposition in any system. It is necessary to include the fission product beta energy and photon production calculated in a subsidiary burnup calculation. In practice, this approach is often neither

appropriate nor possible. The single constant on the AUS library for each actinide, giving the total energy release per fission including an allowance for neutron capture, may be used instead. These values are the ENDF/B-VI Q values (as given in ENDF File 3) plus an allowance for capture heating of 9 MeV per fission.

The value of 9 MeV was derived primarily from HIFAR-like calculations with ^{235}U the only actinide. The fission product beta energy and photon spectrum were taken from the calculation used in the modification of the fission kerma factor. The simple spherical model of HIFAR used for the coupled neutron/photon calculation was poisoned to criticality using either steel or aluminium. The energy deposited in the graphite reflector was not included as it is not cooled by the primary circuit. The total energy release per fission minus the ^{235}U Q value of 193.72 MeV was calculated to be 9.04 and 9.42 MeV with steel and aluminium poisons respectively. A further calculation of a PWR cell was performed as a check. The fission product beta energy and photon spectrum were calculated for a burnup of 30 GWd/t. To ensure that most nuclides included photon production data, the fission products were deleted and poisoning with ^{10}B was used to give criticality. Subtracting the average Q value, obtained by weighting the individual Q values with the fission rates, from the total energy release per fission gave a capture contribution of 8.72 MeV. The variation amounts to less than 0.2% in total energy release so using a constant value of 9 MeV per fission seems reasonable.

Where the total energy release values on the library are not appropriate for a class of calculations, appropriate values may be calculated in some subsidiary calculations and then used by including them in the MIRANDA input. The additional option is:

FER $\quad nuc_1 \;\; fer_1 \;, nuc_2 \;\; fer_2 \;\; \ldots$

where FER is a keyword, the energy release per fission of nuclide nuc_j is set to fer_j and the values may be given in MeV or joules.

3. VALIDATION OF AUS WITH THE ENDFB6 LIBRARY

3.1. General

AUS calculations with the new library *aus/endfb6* have been validated mainly by performing calculations of a wide range of benchmark experiments on thermal and fast reactor assemblies. The specification of the assemblies has been taken mainly from the ENDF-202 compilation [11] but has been supplemented with other experiments in areas of most interest. The specifications are from ENDF-202 except where noted.

Results for AUS calculations of these experiments with ENDF/B-IV data have not been previously published. The results obtained with the previous library AUS.ENDF200G based on ENDF/B-IV have been included here along with published results using ENDF/B-IV data and a few published results using ENDF/B-VI (Rev. 1) data. The inclusion of these results shows the improvement in moving from ENDF/B-IV to ENDF/B-VI and helps to put the current results in context.

The validation of AUS resonance calculations has been previously established by comparison with detailed calculations performed on the same point data files using either collision probability methods [3] or Monte Carlo [12]. In those comparisons, all calculations assumed isotropic scattering in the centre of mass system with constant moderator cross sections. For the lattices studied in the Monte Carlo comparison, AUS overestimated ^{238}U resonance capture by 0.2±0.5 to 1.7±0.4 per cent. This was mainly due to the single mesh per region normally used in the resonance subgroup calculation. These comparisons have not been repeated for ENDF/B-VI since the Monte Carlo program would have to be heavily modified for the new type of point files. Since there have been only minor changes in the generation of the resonance subgroup data from point cross sections, it is expected that errors will be very similar for the ENDF/B-VI based library.

Except where noted, all calculations were done as $S_8 P_3$ transport calculations using the cross sections from MIRANDA in the ANAUSN module [13]. Sufficient groups and mesh were used to ensure a converged result. The ANAUSN transport calculations of lattices were done with circular white boundaries but the square or hexagonal boundary was accounted for in the MIRANDA resonance calculation. All diffusion calculations were performed using the POW3D module [14].

3.2. Thermal Reactor Assemblies

3.2.1. Homogeneous ^{235}U-H_2O benchmarks

The four ORNL homogeneous ^{235}U-H_2O criticals which are included as ENDF benchmarks form a highly accurate set. Results for these benchmarks using ENDF/B-IV have been included in the compilation of results from benchmark testing of ENDF/B-V [15]. Results using ENDF/B-VI (Rev. 1) data have been published by Williams et al [16]. A comparison of the results for k_{eff} are given in Table 3.

Table 3. k_{eff} for Homogeneous ^{235}U-H_2O Benchmarks

Assembly	Measured	ENDF/B-IV ENDF-311†	ENDF/B-IV AUS	ENDF/B-VI Williams [16]	ENDF/B-VI AUS
ORNL-1	1.00026	1.0005±.0014	0.9960	0.9978	0.9971
ORNL-2	0.99975	1.0006±.0009	0.9958	0.9977	0.9970
ORNL-3	0.99994	0.9970±.0015	0.9928		0.9941
ORNL-4	0.99924	0.9982±.0013	0.9943		0.9964
ORNL-10	1.00031	0.9964±.0022	0.9943	0.9973	0.9972

† Average taken from ENDF-311. Range is RMS spread of 4 results.

The AUS results do not include corrections for the deviation of the measured k_{eff} from 1, which are included in the table. Though AUS results were considerably less than the average of other results for ENDF/B-IV, there is quite good agreement between the two sets of ENDF/B-VI results. Good agreement is expected for these very simple assemblies. The agreement with experiment is improved for ENDF/B-VI compared to ENDF/B-IV.

3.2.2. Homogeneous ^{239}Pu-H_2O benchmarks

The ENDF benchmarks include quite a wide range of homogeneous ^{239}Pu-H_2O criticals. A comparison of AUS results and the ENDF-311 compilation of ENDF/B-IV results [15] is given in Table 4.

Table 4. k_{eff} for Homogeneous ^{239}Pu-H_2O Benchmarks

Assembly	H/Pu(fissile)	ENDF/B-IV ENDF-311 *	ENDF/B-IV AUS	ENDF/B-VI AUS
PNL-1	700	1.0215±.0039	1.0167	1.0087
PNL-2	131	1.0185±.0082	1.0122	1.0019
PNL-3	1204	1.0002±.0024	0.9966	0.9903
PNL-4	911	1.0089±.0026	1.0044	0.9969
PNL-5	578	1.0147±.0044	1.0097	1.0010
PNL-6B	131	1.0137±.0032	1.0119	1.0015
PNL-7A	985	1.0141±.0034	1.0140	1.0063
PNL-8A	795	1.0210±.0029	1.0158	1.0078
PNL-9	953	1.0036±.0049	0.9985†	0.9923†
PNL-10	229	1.0094±.0015	1.0030±.0030‡	1.0002±.0020‡
PNL-11	1192	1.0094±.0057	1.0066±.0017‡	1.0010±.0015‡
PNL-12A	1118	1.0056±.0045	1.0139	1.0072

* Average taken from ENDF-311. Range is RMS spread of 5 or 6 results.

† Using RZ diffusion with S_8 P_3 correction of -0.0016 from 1D calc.

‡ Monte Carlo using KENO V.a [17] (P_3 scattering).

Several of the benchmarks have two sets of specifications labelled A or B. The version used in the AUS calculations is indicated in the table but that used by others may differ. There is an unexpectedly large scatter in ENDF/B-IV results from different authors. There is also a large variation in the k_{eff} over the set of experiments. ENDF/B-VI results are clearly better than those with ENDF/B-IV. There are no obvious trends in the results. It appears that there may problems either with the experiments or the ENDF benchmark specifications which contribute to the variation in k_{eff}.

Table 5. Light Water Moderated Benchmark Lattices

			k_{eff}	ρ_{28}	δ_{25}	δ_{28}	C^*
TRX1	Experiment			1.320	0.0987	0.0946	0.797
	Fractional error		0.003	0.016	0.010	0.043	0.009
TRX1	ENDF-311 Nominal	C/E	0.9876	1.047	1.007	1.010	1.011
TRX1-c	AUS ENDF/B-IV	C/E	0.9838	1.073	1.036	1.003	1.022
TRX1-c	AUS ENDF/B-VI	C/E	0.9936	1.033	1.008	1.031	1.002
TRX2	Experiment			0.837	0.0614	0.0693	0.647
	Fractional error		0.001	0.019	0.013	0.05	0.01
TRX2	ENDF-311 Nominal	C/E	0.9935	1.031	0.992	0.975	1.000
TRX2-c	AUS ENDF/B-IV	C/E	0.9890	1.054	1.019	0.969	1.009
TRX2-c	AUS ENDF/B-VI	C/E	0.9960	1.016	0.993	0.999	0.993
TRX3	Experiment			3.030	0.231	0.167	1.255
	Fractional error			0.016	0.013	0.05	0.009
TRX3-r	AUS ENDF/B-IV	C/E	0.9871	1.075	1.073	1.069	
TRX3-r	AUS ENDF/B-VI	C/E	0.9974	1.036	1.043	1.095	1.009
TRX4	Experiment			0.481	0.0358	0.0482	0.531
	Fractional error			0.023	0.014	0.041	0.008
TRX4-r	AUS ENDF/B-IV	C/E	0.9898	1.056	1.001	0.975	
TRX4-r	AUS ENDF/B-VI	C/E	0.9985	1.019	0.979	1.006	0.994
BAPL1	Experiment			1.390	0.084	0.078	
	Fractional error			0.007	0.024	0.05	
BAPL1	ENDF-311 EPRI	C/E	0.9929	1.020	0.986	0.937	
BAPL1	AUS ENDF/B-IV	C/E	0.9869	1.065	1.030	0.940	
BAPL1	AUS ENDF/B-VI	C/E	0.9964	1.026	1.002	0.964	
BAPL2	Experiment			1.120	0.068	0.070	
	Fractional error			0.009	0.015	0.06	
BAPL2	ENDF-311 EPRI	C/E	0.9936	1.054	0.987	0.897	
BAPL2	AUS ENDF/B-IV	C/E	0.9891	1.096	1.035	0.900	
BAPL2	AUS ENDF/B-VI	C/E	0.9972	1.057	1.008	0.924	
BAPL3	Experiment			0.906	0.052	0.057	
	Fractional error			0.011	0.02	0.05	
BAPL3	ENDF-311 EPRI	C/E	0.995	1.024	1.002	0.902	
BAPL3	AUS ENDF/B-IV	C/E	0.9917	1.061	1.038	0.905	
BAPL3	AUS ENDF/B-VI	C/E	0.9986	1.023	1.012	0.931	

Notes:

ρ_{28} — Ratio of epithermal to thermal ^{238}U captures

δ_{25} — Ratio of epithermal to thermal ^{235}U fissions

δ_{28} — Ratio of ^{238}U fissions to ^{235}U fissions

C^* — Ratio of ^{238}U captures to ^{235}U fissions

ENDF-311 Nominal — Nominal results using ENDF/B-IV from ENDF-311

ENDF-311 EPRI — EPRI results using ENDF/B-IV from ENDF-311

3.2.3. Light water moderated benchmark lattices

Table 5 gives results for the two sets of light water moderated benchmarks with 1.3% enriched uranium, which are the TRX lattices with 9.8 mm diameter metal rods and the BAPL lattices with 9.7 mm diameter oxide rods. For TRX1 and TRX2, AUS results are for the cell calculation. AUS calculations for the radial models of these two benchmarks gave values of k_{eff} 0.2% lower. Another anomaly was noted for TRX3 where the calculated δ_{28} was 7% higher at the centre of the radial model than in the cell. That is, an asymptotic spectrum was not achieved. Other reaction ratios for TRX3 were less than 1.5% different in the radial model from those in the cell. The nominal values using ENDF/B-IV from ENDF-311 given for TRX1 and TRX2 represent nominal 'consensus' obtained using what were regarded as the best methods. A 'methods

uncertainty' was also defined in ENDF-311 which represented the scatter resulting from the consistent application of these best methods. The AUS result for the much studied ρ_{28} in TRX1 using ENDF/B-IV is 2.5% higher than the nominal value from ENDF-311 to which a methods uncertainty of 0.4% is attached. The AUS result is more in keeping with the results depicted in Figure 2 of ENDF-311 (page 3-23) which range up to 3.6% above the nominal value and show just one result within ±0.8% of the nominal value. A comparison of the AUS resonance calculation with Monte Carlo for TRX1 [12] showed an overestimate of ^{238}U resonance captures equivalent to 2.2±0.5% in ρ_{28} which makes the Monte Carlo result similar to the nominal result. The AUS ENDF/B-VI results for the TRX ρ_{28} values are only about 1% higher than might be expected on the basis of the bias inferred by the comparison with Monte Carlo. All TRX results using ENDF/B-VI are much improved over those with ENDF/B-IV.

The BAPL lattices have not been looked at so closely. Of the two sets of results included for these lattices in ENDF-311, the EPRI results using ENDF/B-IV have been included in the table though EPRI had higher than the average results for k_{eff} in the TRX lattices using ENDF/B-V. The AUS results using ENDF/B-VI appear to be consistent with the results for the TRX lattices.

3.2.4. The R/100 light water moderated lattices

The R/100 experiments [18] on 3% enriched uranium rods of 10 mm diameter have been studied by a number of authors [19] [20] [21]. Unfortunately, the experimental results quoted for these lattices show some variation. Reference 18 has been used here. The AUS results using ENDF/B-IV and ENDF/B-VI are given in Table 6.

Table 6. R/100 Light Water Moderated Lattices

		k_{eff}	RCR	FFR	Pu9/U5	Lu/Mn	Cool/Fuel	Clad/Fuel
R3	Expt		4.789	0.1066	1.661	1.112	1.223	1.097
R3	FSD	0.0012	0.011	0.017	0.006	0.008	0.013	0.009
R3	AUS IV	0.9843	1.079	0.935	1.019	0.971	0.960	1.000
R3	AUS VI	0.9971	1.046	0.956	1.008	1.099	0.962	1.001
R1	Expt		4.158	0.0858	1.589	1.160	1.260	1.130
R1	FSD	0.001	0.007	0.01	0.006	0.005	0.012	0.008
R1	AUS IV	0.9886	1.067	0.976	1.021	0.981	0.950	0.974
R1	AUS VI	0.9991	1.035	1.000	1.010	1.084	0.952	0.975
R1H	Expt		4.293	0.0895	1.637	1.241	1.233	1.120
R1H	FSD	0.0016	0.011	0.03	0.006	0.006	0.011	0.008
R1H	AUS IV	0.9854	1.060	0.955	1.029	0.991	0.960	0.978
R1H	AUS VI	0.9966	1.028	0.977	1.018	1.099	0.962	0.979
R2	Expt							
R2	FSD	0.0021						
R2	AUS IV	1.0007						
R2	AUS VI	1.0040						

Notes:

FSD	Fractional standard deviation on experiment
AUS IV	Calc/Expt for AUS with ENDF/B-IV library
AUS VI	Calc/Expt for AUS with ENDF/B-VI library
RCR	Ratio of ^{238}U captures to ^{235}U fissions relative to thermal
FFR	Ratio of ^{238}U to ^{235}U fissions
Pu9/U5	Ratio of ^{239}Pu to ^{235}U fissions relative to thermal
Lu/Mn	Ratio of ^{176}Lu to ^{55}Mn captures relative to thermal
Cool/Fuel	Ratio of ^{235}U fissions in coolant to fuel
Clad/Fuel	Ratio of ^{235}U fissions in clad to fuel
R1H	As R1 but 60K hotter

Experimental error on k_{eff} of R1H relative to R1 is ±0.0014

The results with ENDF/B-VI show an apparent trend in k_{eff} with lattice pitch, which takes the values 12.506, 13.2 and 18.66 mm for R3, R1 and R2 respectively. The RCR is overestimated by more than would be expected from the δ_{28} for TRX and BAPL. However, it has been suggested that the experimental results should be increased by 2 to 3% [21]. The variation of k_{eff} with temperature has improved slightly in going from ENDF/B-IV to ENDF/B-VI. Thus the variation in ^{235}U thermal η introduced in ENDF/B-VI has had only a small effect on the overestimate of temperature coefficient for these lattices. The deterioration in the Lu/Mn ratio is a consequence of a change in the parameters of the first ^{55}Mn resonance in ENDF/B-VI which results from an improved measurement of this resonance. Presumably, there is also an error in the ^{176}Lu data which used to compensate.

3.2.5. Heavy water moderated benchmark lattices

The ENDF benchmarks used to include a set of 23.65 mm natural uranium rods in heavy water labelled MIT1 to MIT3. These were replaced by the set of 9.83 mm 1.3% enriched uranium rods labelled MIT4 to MIT6. Neither set has been given much attention in compilations of benchmark testing. Results for both sets are given in Table 7. The bucklings inferred from reaction rate measurements specified in the MIT4 to MIT6 benchmarks were not used. It is bizarre to use such bucklings and thus normalise to 20 year old data and methods. The experimental bucklings (9.55, 12.44 and 10.41 m^{-2} for 4 5 6 respectively) were used instead. The ENDF/B-VI k_{eff} results for MIT1-3 are quite good but the MIT4-6 results are poor. This is considered further below. The reaction rate comparison shows that the results for ρ_{28} and C^* are inconsistent. The ρ_{28} results for MIT4-6 are not believable. It is concluded that neither set of lattices is suitable as a benchmark.

Table 7. Heavy Water Moderated Benchmark Lattices

			k_{eff}	ρ_{28}	δ_{25}	δ_{28}	C^*
MIT1	Experiment			0.498	0.0447	0.0597	1.017
	Fractional error		0.016	0.043	0.033	0.023	
MIT1	ENDF-230 CRNL†	C/E	0.9829	1.010	1.12	0.898	
MIT1	AUS ENDF/B-IV	C/E	0.9803	1.066	1.070	0.970	0.985
MIT1	AUS ENDF/B-VI	C/E	0.9962	1.013	1.037	1.006	0.953
MIT2	Experiment			0.394	0.031	0.0596	0.948
	Fractional error		0.005	0.1	0.029	0.020	
MIT2	ENDF-230 CRNL†	C/E	0.9829	1.033	1.29	0.856	
MIT2	AUS ENDF/B-IV	C/E	0.9797	1.108	1.262	0.936	0.981
MIT2	AUS ENDF/B-VI	C/E	0.9951	1.052	1.223	0.976	0.967
MIT3	Experiment			0.305	0.0248	0.0583	0.859
	Fractional error		0.013	0.4	0.020	0.019	
MIT3	ENDF-230 CRNL†	C/E	0.9850	1.021	1.23	0.835	
MIT3	AUS ENDF/B-IV	C/E	0.9806	1.118	1.295	0.924	1.016
MIT3	AUS ENDF/B-VI	C/E	0.9954	1.060	1.181	0.967	1.004
MIT4	Experiment			1.155	0.0865	0.0459	1.007
	Fractional error		0.001	0.018	0.028	0.008	
MIT4	AUS ENDF/B-IV	C/E	0.9716	1.010	0.974	0.828	1.008
MIT4	AUS ENDF/B-VI	C/E	0.9893	0.975	0.950	0.848	0.991
MIT5	Experiment			0.525	0.0371	0.0326	0.740
	Fractional error		0.004	0.032	0.03	0.01	
MIT5	AUS ENDF/B-IV	C/E	0.9861	0.995	0.996	0.813	0.993
MIT5	AUS ENDF/B-VI	C/E	1.0019	0.955	0.971	0.841	0.981
MIT6	Experiment			0.317	0.0222	0.0291	0.647
	Fractional error		0.006	0.11	0.06	0.003	
MIT6	AUS ENDF/B-IV	C/E	0.9904	0.964	0.970	0.794	0.984
MIT6	AUS ENDF/B-VI	C/E	1.0048	0.924	0.946	0.829	0.976

† Chalk River results using ENDF/B-IV from ENDF-230

3.2.6. Other heavy water moderated lattices

Tables 8 and 9 give results for 47 lattices with uranium rods in heavy water. All but the four Saclay oxide rods are metal, and all but the three MIT rods are natural uranium. The specifications of the Saclay and Savannah River lattices were taken from the compilation of Rose [22], and those for the ZEEP lattices from Craig [20]. Also included in the table are the calculated ratios of epithermal ^{238}U captures to total ^{235}U fissions. A plot of k_{eff} versus this ratio given in Figure 1 shows a clear trend in spite of the large scatter. A linear least squares fit yields

$$k_{eff} = (1.0037 \pm 0.001) - (0.0162 \pm 0.0035) \times \text{ratio} \quad .$$

MIT4 is well off the trend line. The ZEEP lattices proposed [20] as a benchmark give a consistent set of results which well match the overall trend. Therefore, the use of the ZEEP lattices as a benchmark is endorsed, though the range is rather limited. The calculated C/E for ZEEP1 RCR and δ_{28} were 1.016±0.004 and 1.001±0.021 respectively.

Table 8. Uranium Rods in Heavy Water — Saclay

Pitch (square)	EU8C†	k_{eff} ENDF/B-IV	k_{eff} ENDF/B-VI	
				Saclay 29.2 mm metal rod
12.00	0.322	0.9808	0.9969	
13.00	0.278	0.9847	1.0003	
15.00	0.218	0.9858	1.0008	
17.00	0.179	0.9839	0.9983	
19.00	0.153	0.9843	0.9981	
21.00	0.134	0.9855	0.9989	
				Saclay 35.6 mm metal rod
13.00	0.382	0.9831	1.0002	
15.00	0.297	0.9815	0.9978	
17.00	0.242	0.9824	0.9981	
19.00	0.205	0.9848	0.9999	
21.00	0.179	0.9850	0.9996	
23.00	0.161	0.9853	0.9986	
25.00	0.149	0.9837	0.9973	
				Saclay 44.0 mm metal rod
13.00	0.545	0.9782	0.9971	
15.00	0.418	0.9768	0.9948	
17.00	0.337	0.9784	0.9957	
19.00	0.283	0.9803	0.9969	
21.00	0.245	0.9828	0.9988	
23.00	0.219	0.9825	0.9980	
25.00	0.201	0.9818	0.9968	
27.00	0.188	0.9834	0.9979	
29.00	0.177	0.9880	1.0021	
30.00	0.174	0.9851	0.9991	
				Saclay 46 mm oxide rod
15.00	0.293	0.9886	1.0020	
17.00	0.233	0.9890	1.0019	
19.00	0.193	0.9918	1.0043	
21.00	0.166	0.9907	1.0027	

† Ratio of epithermal ^{238}U captures to ^{235}U fissions calculated using ENDF/B-VI.

Table 9. Uranium Rods in Heavy Water — others

Pitch (square)	EU8C†	k_{eff} ENDF/B-IV	k_{eff} ENDF/B-VI	
				Savannnah River 25.3 mm rod
7.60	0.616	0.9832	1.0007	
10.20	0.345	0.9829	0.9989	
12.70	0.232	0.9860	1.0009	
14.15	0.193	0.9865	1.0010	
16.47	0.151	0.9893	1.0030	
18.89	0.124	0.9877	1.0008	
19.08	0.122	0.9908	1.0039	
21.31	0.106	0.9925	1.0051	
22.06	0.102	0.9943	1.0067	
23.64	0.095	0.9940	1.0060	
28.66	0.053	0.9960	1.0071	
				MIT 25.65 mm rod
10.64	0.325	0.9803	0.9962	MIT1
11.82	0.269	0.9797	0.9951	MIT2
13.59	0.211	0.9806	0.9954	MIT3
				MIT 10 mm rod (0.95% enrich)
3.55	0.528	0.9716	0.9893	MIT4
5.32	0.243	0.9861	1.0019	MIT5
7.09	0.143	0.9904	1.0048	MIT6
				ZEEP 32.57 mm rod
18.61	0.185	0.9880	1.0009	
13.00	0.333	0.9844	0.9993	
11.22	0.437	0.9804	0.9986	

† Ratio of epithermal ^{238}U captures to ^{235}U fissions calculated using ENDF/B-VI.

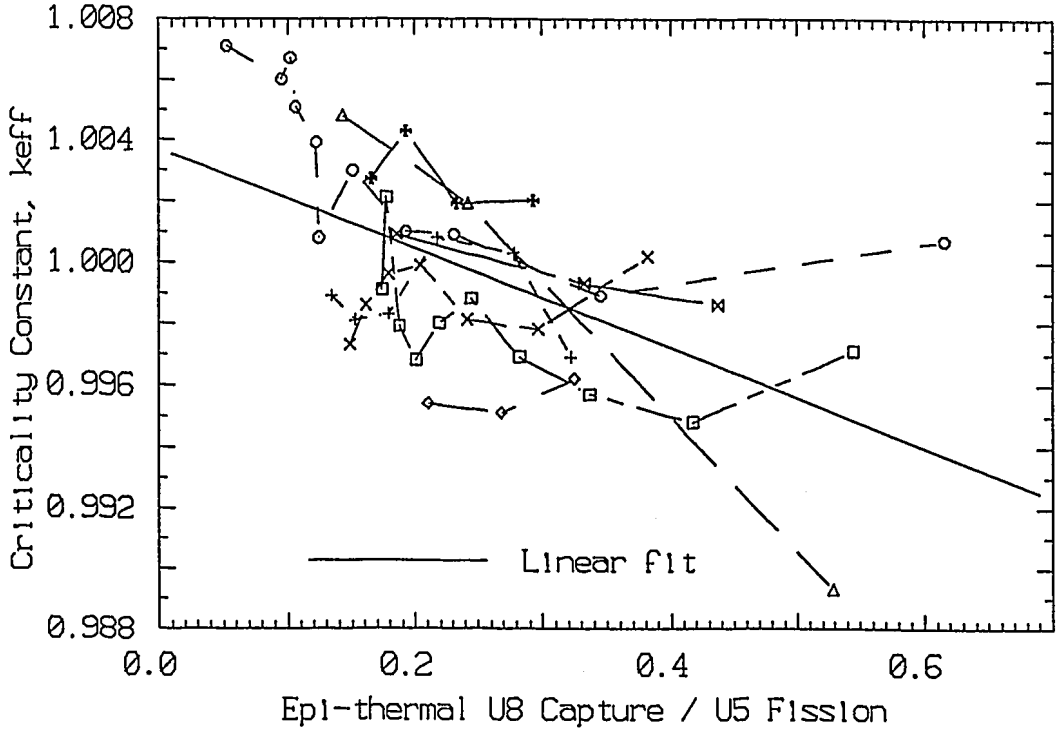

Figure 1. k_{eff} Versus Epi-thermal ^{238}U Captures for Uranium Rods in D_2O

3.3. Fast Reactor Benchmarks

The ENDF-202 compilation of fast reactor benchmarks [11] includes a wide range of mostly older fast critical experiments which have been represented by fairly simple specifications. They are therefore very suitable for general validation of non-thermal data though of less value in assessing validity for calculations of modern fast reactor concepts.

The AUS library allows for only a single fission spectrum for each nuclide and the weighting used in the formation resulted in thermal fission spectra for the fissile nuclides. The effect of this was checked for several assemblies by using a fission spectrum for the fissile nuclide weighted with the flux spectrum for that assembly. (The procedure used was too clumsy for normal use.) The results are given in Table 10.

Table 10. Effect of Fission Spectrum Weighting

Assembly	δ k_{eff}	Change in $^{238}U/^{235}U$ fissions (%)	
GODIVA	+0.0014	+1.5	
JEZEBEL	+0.0020	+1.6	
ZPR-6-7	+0.0019	+1.7	(using JEZEBEL spectrum)
ZPR-6-7	+0.0005	+0.4	
VERA-11A	+0.0008		

In view of these results, standard fission spectra were used in the benchmarks except that the GODIVA ^{235}U spectrum was used for GODIVA and FLATTOP-25, and the JEZEBEL ^{239}Pu spectrum was used for JEZEBEL and JEZ-PU(20.1).

In calculating previous results using ENDF/B-IV data, diffusion theory was used where specified in ENDF-202 and P_0 scattering with a transport cross section was used in the S_N calculations. The transport cross sections for blankets came directly from the library. For the reactor cores, a B_1 calculation was used to give neutron currents then the current weighted inscatters were subtracted from the total to give the transport cross section. This procedure was checked for the ENDF/B-VI data by comparison with S_N P_3 calculations and it was found that the previous procedure was inadequate. A comparison of the resulting k_{eff} is included with the main results given in Table 12. The correction column gives the correction applied to the final ENDF/B-VI k_{eff} to account for heterogeneity and S_N error which were taken from ENDF-230 [23]. The two columns giving ENDF/B-IV and ENDF/B-VI results using the previous procedure also include diffusion corrections taken from ENDF-230 for four assemblies . On the basis of this work in which S_8 P_3 was used for the four assemblies, these corrections appear to be wrong because of the use of a transport approximation in the S_N calculation. The differences in k_{eff} between the S_N and diffusion calculations are given in Table 11.

Table 11. Correction to k_{eff} for Diffusion Calculations

Assembly	ENDF-230	This work
ZPR-3-48	+0.0072	+0.0029
ZPR-6-7	+0.0016	-0.0003
ZPR-6-6A	+0.0013	-0.0006
ZPPR-2	+0.0024	+0.0016

This result is surprising as the diffusion calculations tend to be more accurate than the S_N calculations with a transport cross section. However, these results are consistent with differences between use of a transport cross section and P_3 scattering obtained for the other assemblies (Table 12).

The results for k_{eff} are much improved over the ENDF/B-IV results, but VERA-11a is an exception. These results differ markedly from published results [24] using ENDF/B-VI for a subset of these assemblies which are also included in Table 12. The values for k_{eff} in the current work are closer to unity. The major differences are in assemblies with significant ^{238}U resonance captures. This is supported by a comparison of ^{238}U captures to ^{235}U fissions, which are included with the fission ratios in Table 13, with those of reference 23. Also included as Table 14 are some calculated worths, but the ENDF/B-IV reactivity scales taken from ENDF-230 were used. They are thus best thought of as giving relative worths only.

These results provide a general validation of the non-thermal data on the AUS library. There are surprising differences in ENDF/B-VI results obtained for some of these assemblies. It is thought that some of the

Table 12. k_{eff} for Fast Reactor Benchmarks

Benchmark	F28/F25 (Expt)	k_{eff} Corr.†	k_{eff} for Various AUS Calculations ENDF/B-IV‡	ENDF/B-VI‡	ENDF/B-VI	k_{eff} W&W [24] ENDF/B-VI
JEZEBEL	0.2137				0.9983	0.9991
JEZ-PU(20)	0.2065				0.9985	0.9943
GODIVA	0.1647				0.9975	0.9974
FLATTOP-25	0.1488				1.0017	1.0062
ZPR-3-6F	0.078	-0.0038	1.0113	1.0062	1.0010	
VERA-11A	0.077	-0.0024		0.9898	0.9829	
VERA-1B	0.0665	-0.0010	0.9964	1.0000	0.9952	
ZPR-3-12	0.047	-0.0018	1.0043	1.0083	1.0042	1.0160
ZEBRA-3	0.0461	-0.0010	0.9986	1.0045	1.0001	
SNEAK-7A	0.0448		0.9983	1.0068	1.0030	
ZPR-3-11	0.0380	-0.0013	1.0096	1.0060	1.0026	1.0215
BIGTEN	0.0373				0.9988	1.0208
SNEAK-7B	0.0330		0.9933	1.0051	1.0020	
ZPR-3-48	0.0321	+0.0183	0.9987	1.0108	1.0065	
ZEBRA-2	0.0320	-0.0005	0.9915	1.0052	1.0031	
ZPR-3-56B	0.0308	-0.0055	0.9806	0.9978	0.9940	
ZPR-6-6A	0.0241	+0.0073	0.9904	1.0087	1.0068	1.0141
ZPR-6-7	0.0220	+0.0167	0.9900	1.0089	1.0069	1.0153
ZPPR-2	0.0201	+0.0175	0.9894	1.0039	1.0032	

F28/F25 — Ratio of ^{238}U to ^{235}U fissions

† Corrections from ENDF-230.

‡ Using diffusion theory and diffusion corrections or transport approximation.

Table 13. Calc/Expt for Central Reaction Rates Relative to ^{235}U

Benchmark	Fission Ratios ^{239}Pu	^{238}U	^{240}Pu	^{237}Np	^{234}U	^{236}U	Capture ^{238}U
JEZEBEL	0.983	0.973		0.991			
JEZ-PU(20)	0.970		1.014				
GODIVA	0.987	0.967		0.977			
FLATTOP-25	0.995	0.980		1.006			
ZPR-3-6F	1.030	0.992	1.036		1.138		0.932
VERA-11A	1.094	1.194	1.142	1.193			
VERA-1B	1.062	1.161	1.205	1.187		1.245	0.995
ZPR-3-12	0.995	1.049			1.132		0.957
ZEBRA-3	1.004	1.028	1.094	1.075	1.122	1.133	
SNEAK-7A	0.964	0.959					0.964
ZPR-3-11	0.996	1.060	1.108	1.053	1.161	0.816	0.960
BIGTEN	0.998	1.043		1.070			0.985
SNEAK-7B	0.989	1.013					0.997
ZPR-3-48		1.053					0.951
ZEBRA-2	0.998	1.022	1.092	1.071	1.504	0.824	0.944
ZPR-3-56B	0.950	0.999	0.893		1.156	1.123	
ZPR-6-6A		0.952					1.001
ZPR-6-7	0.965	0.972					1.018
ZPPR-2	0.983	1.107	1.159		1.158	1.215	

discrepancies with experiment are due to limitations of the experiments and the simple representations used in the benchmark specifications.

Table 14. Calc/Expt for Central Material Worths

	^{239}Pu	^{235}U	^{238}U	^{10}B	Na	Fe	Cr	Ni	Mo
ZEBRA-3	1.175	1.128	1.073	1.002	1.296				
ZPR-3-11	1.051	1.063	0.947	0.964	1.516	1.196	1.295	1.420	1.188
ZPR-3-48	1.158	1.143	1.034	0.992	2.192	1.234	1.351	1.407	1.437
ZEBRA-2	1.065	1.076	1.031	0.918	2.079	1.299	1.327	1.019	
ZPR-6-6A	1.008	1.029	1.085	0.930	1.781				
ZPR-6-7	1.121	1.083	0.948	1.066	1.080	1.059	1.170	1.169	1.417
	Mn	Al	O	C	Au	Cu	H	^{240}Pu	
ZEBRA-3		1.130		1.109	1.075	1.131	1.426		
ZPR-3-11	1.251	1.257	0.939	1.114					
ZPR-3-48	1.440	1.380		4.162					
ZEBRA-2	1.848	1.198		0.720	1.527	1.415	0.939	0.327	
ZPR-6-6A				0.868					
ZPR-6-7		1.298		1.313					

3.4. Other Validation

Other validation has been very limited. The analysis of fission kerma did lead to the correction of a number of errors introduced into the photon production data. That analysis provided some qualitative validation of the photon production data for the most common reactor materials. It also provided some validation of the inclusion of the photon interaction data. In particular, checks were made that the photon energy deposited from fission product photons matched the emitted photon energy. It is concluded that there should be no gross errors remaining in energy release, photon production, and photon interaction data.

4. LIBRARY CONTENT AND USAGE

The set of nuclides, excluding fission products, currently included in the *aus/endfb6* library is given in Table 15. Each nuclide has a three part name. The first part gives the simple name and the remainder describes the origins of the nuclide. The nuclide labelled *zz999* is a pure absorber with inverse velocity energy dependence and a cross section of 1 barn at 0.025 eV. The nuclides named *h0zrh* and *zr0zrh* are H and Zr in Zr-H. Some nuclides are identical on ENDF/B-V (part of which was included on AUS.ENDF200G) and ENDF/B-VI. This is indicated by the second part of the full nuclide name being *endfb5*. The third part of the name for ENDF/B-V nuclides is used to indicate that the AUS cross sections were not reprocessed (*orig*) or were reprocessed by using NJOY (*njoy*). For ENDF/B-VI nuclides, the third part of the name indicates the ENDF/B-VI revision number and any AUS revision number. The ENDF/B-VI files correspond to revision 1 of the whole file and the revised nuclides are thus denoted *m010* for simple isotopes or *m0n0* for elements in which n constituents have been revised. The last character is reserved for AUS revisions.

The representation of any nuclide on the library is at least as detailed as on the previous AUS library in terms of representation of P_l expansion, temperature effects, resonance shielding and photon data. The P_l order given in the table is for fast neutron scattering. Thermal neutron scattering and photon production have a P_3 expansion at most. The photon interaction has a P_5 expansion for all data given. The nuclides with resonance treatment are indicated in the table; the remainder are for infinite dilution. The table indicates those nuclides without photon data. Such nuclides also have no kerma data. Users should take care that the data on the library are appropriate for the intended use. In particular, fission products have neutron cross sections only, no energy deposition and no thermal scattering. Their scattering expansion is P_1.

The library includes additional cross sections for many of the lighter nuclides. The previous libraries just included (n,γ) and (n,2n), except for some nuclides where another reaction was given instead. Now there is a set of reactions which should satisfy all requirements (except for individual reactions of an isotope included in an element). These reactions include (n,p), (n,α), gas production and neutron damage.

On the *photon* computer at Ansto, further information on a nuclide may be obtained using the *plotxs* command, which enables any cross sections on the library to be plotted interactively. The command also lists the set of additional reactions and any comments on a requested nuclide. The reactions are identified by ENDF MT numbers. Some of these are:

16	(n,2n)		
102	(n,gamma)		
103	(n,p)	203	total proton production (H gas)
105	(n,t)	205	total tritium production
107	(n,alpha)	207	total alpha production (He gas)
444	total damage energy		

If further detail on the generation of any nuclide *xyz* is required, the input files used may be accessed on the *photon* as files *xyz.** in the directory */home/gsr/work/xs6*. For further information on the neutron cross section data, the original ENDF/B-VI files may be accessed as individual files for each material in the directory */home/gsr/xs/endfb6/neutron*.

The additional reactions may be accessed within AUS by using MIRANDA to set one of the output reactions to the desired MT number. Derived AUS cross section files still only have cross sections for nine reactions. The additional input keyword in MIRANDA is:

SETREAC irn mtn (list of library nuclides)

where irn is the AUS output reaction number (<10), and mtn is the MT value.
A number of SETREAC entries can be included. The cross section will be set to zero for those nuclides which don't have cross sections for mtn. Getting sensible resultant cross sections, particularly for mixtures, is the responsibility of the user.

The set of fission products has been increased from that used previously by 2 to 158. The additional ones are ^{105}Ru and ^{157}Eu. The number of fission products in the main set to be used with the pseudo product PFP was increased by the 8 nuclides ^{85}Kr, ^{90}Sr, ^{105}Ru, ^{106}Ru, ^{135}I, ^{137}Cs, ^{151}Pm and ^{157}Eu. The complete set is given in Table 16.

5. CONCLUSION

The cross section library *aus/endfb6* with 200 neutron and 37 photon energy groups has been generated from revision 1 of ENDF/B-VI for use within the AUS neutronics code system. It should be suitable for calculations of all types of nuclear reactors and many other neutron applications. The validity of AUS with this library has been established for a wide range of thermal and fast reactor benchmark experiments. The comprehensive results obtained from a consistent set of calculations of these experiments should also assist in assessing the capability of the ENDF/B VI files. However, the usefulness of these results in this respect is reduced by apparent deficiences in the ENDF compilation of benchmarks which formed the bulk of the experiments considered. The performance of the library is clearly superior to the previous AUS library based on ENDF/B-IV.

6. REFERENCES

(1) Robinson, G.S. [1987] - A guide to the AUS modular neutronics code system. AAEC/E645.

(2) Robinson, G.S. [1985] - MIRANDA - a module based on multiregion resonance theory for generating cross sections within the AUS neutronics code system. AAEC/E626.

(3) Robinson, G.S. [1977] - AUS module MIRANDA - a data preparation code based on multiregion resonance theory. AAEC/E410.

(4) NJOY91.38 [1992] - A code system for producing pointwise and multigroup neutron and photon cross sections from ENDF/B evaluated nuclear data. ORNL/RSIC/PSR-171.

(5) MacFarlane, R.E., Muir, D.W. & Boicourt, R.M. [1982] - The NJOY nuclear data processing system. LA-9303-M (ENDF-324).

(6) US National Nuclear Data Center [1992] - ENDF/B-6 - The U.S. evaluated nuclear data library for neutron reaction data. IAEA-NDS-100, Rev. 4.

(7) Cullen, D.E. & McLaughlin, P.K. [1989] - The 1989 ENDF pre-processing codes. IAEA-NDS-39, Rev. 5.

[8] Rose, P.F. & Dunford, C.L. [1990] - ENDF-102 - Data formats and procedures for the evaluated nuclear data file ENDF-6. BNL-NCS-44945.

[9] Harrington, B.V. [1976] - AUS module AUSED - an editing program for AUS cross section data pools. AAEC/E389.

[10] Robinson, G.S. [1986] - CHAR and BURNMAC - burn-up modules of the AUS neutronics code system. AAEC/E624.

[11] ENDF-202 [1974] - Cross section evaluation working group benchmark specifications. BNL 19302. (With revisions to Sept, 1991).

[12] Robinson, G.S. [1985] - A comparison of neutron resonance absorption in thermal reactor lattices in the AUS neutronics code system with Monte Carlo calculations. AAEC/E614.

[13] Clancy, B.E. [1982] - ANAUSN - a one-dimensional multigroup SN transport theory module for the AUS reactor neutronics system. AAEC/E539.

[14] Unpublished extension of POW module :
Pollard, J.P. [1974] - AUS module POW - a general purpose 0,1 and 2D multigroup neutron diffusion code including feedback-free kinetics. AAEC/E269.

[15] ENDF-311 [1982] - Benchmark data testing of ENDF/B-V. BNL-NCS-31531.

[16] Williams, M.L., MacFarlane, R.E., Milgram, M., Wright, R.Q. & Kahler, A.C. [1991] - Initial data testing of ENDF/B-VI for thermal reactor benchmark analysis. Trans. Am. Nuc. Soc., 64, 561.

[17] Petrie, L.M. & Landers, N.F. [1984] - KENO V.a - An improved Monte Carlo criticality program with supergrouping. ONRL/NUREG/CSD-2/V1/R2.

[18] Brown, W.A.V, Fox, W.N., Skillings, D.J., George. C.F. & Burholt, G.D. [1967] - Measurements of material buckling and detailed reaction rates in a series of low enrichment UO_2 fuelled cores moderated by light water. AEEW-R502.

[19] Kemshell, P.B. [1972] - Some integral properties of nuclear data deduced from WIMS analyses of well thermalised uranium lattices. AEEW-R786.

[20] Craig, D.S. [1984] - Testing ENDF/B-V data for thermal reactors. AECL-7690 (Rev. 1).

[21] Donnelly, J.V. [1988] - Validation of WIMS with ENDF/B-V data for pin-cell lattices. AECL-9564.

[22] Rose, E.K. [1970] - A study of some heavy water moderated natural uranium systems using the WIMS code. AAEC/TM553.

[23] ENDF-230 [1976] - Benchmark testing of ENDF/B-IV. BNL-NCS-21118.

[24] Wright, R.Q. & White, J.E. [1991] - Fast reactor data testing of ENDF/B-VI at ORNL. Trans. Am. Nuc. Soc., 64, 566.

Table 15. Nuclides in the AUS ENDFB6 Library

Name	Source		Pl order	Temperature range	Resonance data?	Photon data?
zz999	njoy	orig	-			No
ch2	endfb6	m020	7	296		
h2o	endfb6	m010	7	296-1000		
h0zrh	endfb6	m010	7	296-1000		
d2o	endfb6	orig	7	296-1000		
he3	endfb6	m010	3	296		No
li6	endfb6	m010	7	296		
li7	endfb6	orig	7	296		
be	endfb6	orig	7	296-1000		
b10	endfb6	m010	7	296		
b11	endfb6	orig	7	296		
c	endfb6	m010	7	296-1600		
n	endfb6	orig	7	296		
o	endfb6	orig	7	296-3000		
na	endfb6	m010	7	296	Yes	
mg	endfb5	njoy	3	296		
al	endfb5	njoy	7	296	Yes	
si	endfb5	orig	7	296		
cl	endfb5	njoy	3	296		
ca	endfb5	njoy	7	296		
ti	endfb5	orig	3	296		
v	endfb6	orig	3	296		
cr	endfb6	m040	7	296	Yes	
mn	endfb6	orig	3	296	Yes	
fe	endfb6	m040	7	296	Yes	
co	endfb6	orig	3	296		
ni	endfb6	m050	7	296	Yes	
cu	endfb6	orig	3	296		
ga	endfb5	njoy	1	296		No
zr	endfb6	m010	7	296-1000	Yes	
zr0zrh	endfb6	m010	7	296-1000	Yes	
nb	endfb6	orig	3	296		
mo	endfb5	orig	3	296		
cd	endfb5	orig	3	296		
ba	endfb5	njoy	1	296		
gd	endfb5	njoy	1	296		No
er166	endfb6	orig	1	296		No
er167	endfb6	orig	1	296		No
lu176	endfb5	njoy	1	296		No
au	endfb6	m010	1	296		No
pb	endfb6	m010	7	296	Yes	
bi	endfb6	orig	7	296	Yes	
u234	endfb6	orig	3	296-900	Yes	
u235	endfb6	m010	7	296-2100	Yes	
u236	endfb6	orig	3	296-900	Yes	
u237	endfb6	orig	3	296		
u238	endfb6	m010	7	296-2100	Yes	
np237	endfb6	m010	3	296		
np239	endfb6	orig	3	296		
pu238	endfb6	orig	3	296		
pu239	endfb6	orig	3	296-2100	Yes	
pu240	endfb6	m010	3	296-2100	Yes	

Name	Source		Pl order	Temperature range	Resonance data?	Photon data?
pu241	endfb6	m010	3	296-2100	Yes	
pu242	endfb6	orig	3	296-2100	Yes	
am241	endfb6	orig	3	296		
am242m	endfb6	m010	3	296		
am242	endfb6	m010	3	296		
am243	endfb6	orig	3	296		
cm242	endfb6	orig	3	296		
cm243	endfb5	njoy	3	296		
cm244	endfb5	njoy	3	296		
cm245	endfb6	orig	3	296		

Table 16. Fission Products in the AUS ENDFB6 Library

	Mass Numbers and possible Isomeric State for each element	
Element	Normal Set	Extended Set
ge		72 73 74 76
as		75
se		76 77 78 80 82
br		81
kr	83 85	82 84 86
rb		85 87
sr	90	86 88 89
y		89 91
zr	95	90 91 92 93 94 96
nb	95	
mo	95	96 97 98 99 100
tc	99	
ru	100 101 102 103 105 106	104
rh	103 105	
pd	104 105 106 107 108	110
ag	109	111
cd	113	110 111 112 114 115m 116
in		115
sn		116 117 118 119 120 122 123 124 126
sb		121 123 124 125
te		122 123 124 125 126 127m 128 129m 130 132
i	135	127 129 131
xe	131 133 135	128 130 132 134 136
cs	133 134 135 137	136
ba		134 136 137 138 140
la		139 140
ce	144	140 141 142 143
pr	143	141
nd	143 144 145 146 147 148	142 150
pm	147 148m 148 149 151	
sm	147 149 150 151 152	148 153 154
eu	153 154 155 157	156
gd	157	154 155 156 158 160
tb		159 160
dy		160 161 162 163 164
ho		165